Biochemical and Biophysical Research Communications 515 (2019) 248–253

Contents lists available at ScienceDirect

Biochemical and Biophysical Research Communications

journal homepage: www.elsevier.com/locate/ybbrc

N-Substituted amino acid inhibitors of the phosphatase domain of the soluble epoxide hydrolase

Naoki Matsumoto [a, b], Masaki Kataoka [a], Hibiki Hirosaki [a], Christophe Morisseau [b], Bruce D. Hammock [b], Eriko Suzuki [a], Keiji Hasumi [a, *]

[a] Department of Applied Biological Science, Tokyo Noko University, Tokyo, 183-8509, Japan
[b] Department of Entomology and Nematology, U.C.D. Comprehensive Cancer Center, One Shields Avenue, University of California Davis, Davis, CA, 95616, USA

ARTICLE INFO

Article history:
Received 23 April 2019
Accepted 12 May 2019
Available online 27 May 2019

Keywords:
Soluble epoxide hydrolase
Phosphatase
Inhibitor

ABSTRACT

The soluble epoxide hydrolase (sEH) is a bifunctional enzyme implicated in the regulation of inflammation. The N-terminal domain harbors a phosphatase activity (N-phos) with an affinity to lipid phosphomonoesters, and the C-terminal domain has an activity to hydrolyze anti-inflammatory lipid epoxides (C-EH). Although many potent inhibitors of C-EH have been discovered, little is known about inhibitors of N-phos. Here, we identify *N*-substituted amino acids as selective inhibitors of N-phos. Many of the *N*-substituted amino acids inhibited differently mouse and human N-phos; phenylalanine derivatives are relatively selective for mouse N-phos, whereas tyrosine derivatives are more selective for human N-phos. The best inhibitors, Fmoc-L-Phe(4-CN) (**67**) and Boc-L-Tyr(Bzl) (**23**), inhibited mouse and human N-phos competitively with K_I in the low micromolar range. These compounds inhibit the N-phos activity 37- (**67**) and 137-folds (**23**) more potently than the C-EH. The differences in inhibitor structure activity suggest different active site structure between species, and thus, probably a divergent substrate preference between mouse and human N-phos.

1. Introduction

The soluble epoxide hydrolase (sEH) is conserved among animal species. In mammals, sEH exists as a homodimer, in which each subunit is composed of two distinct domains [1]. The C-terminal domain has an epoxide hydrolase activity (C-EH), which hydrolyzes endogenous signaling molecules, epoxy-fatty acids [1]. C-EH is a promising therapeutic target of several diseases including inflammation, neurological disorders, and pain [2,3]. The N-terminal domain harbors a phosphatase activity (N-phos), which hydrolyzes lipophilic phosphomonoesters such as lysophosphatidic acids [4,5], sphingosine 1-phosphate [4,5], and isoprenoid phosphates/pyrophosphates [6,7]. While the involvement of N-phos in endothelial nitric oxide signaling [8,9] and cholesterol synthesis regulation [10,11] has been reported, no consensus has been reached on its physiological roles [12]. One of the major limitations to pursue the function of *N*-phos is the lack of a selective inhibitor. Although several N-phos inhibitors, including alkyl sulfates, sulfonates, and phosphonates [6], ebselen (an organoselenium) [13], oxaprozin (a non-steroidal analgesic) [14], SMTPs [15–17], and lipophilic N-acetylcysteine derivatives [10], have been identified, most of them are not selective for N-phos. *N*-Acetyl-*S*-farnesyl-L-cysteine (AFC) is one of the best inhibitors found so far with respect to potency and selectivity, based on the studies using human sEH [10]. However, we found that AFC inhibited C-EH of mouse as well as its N-phos activity.

Here, we investigate the ability of a variety of *N*-substituted amino acids to inhibit N-phos and C-EH in human and mouse sEH. For the best compounds, their mechanism of action was investigated. Finally, the molecular source of the difference in inhibitor selectivity was examined and is discussed in terms of difference in N-phos substrate preference across species.

Abbreviations: sEH, soluble epoxide hydrolase; C-EH, C-terminal epoxide hydrolase; N-phos, N-terminal phosphatase; AFC, *N*-acetyl-*S*-farnesyl-L-cysteine; AttoPhos, 2'-[2-benzothiazoyl]-6'-hydroxybenzothiazole phosphate; PHOME, (3-phenyl-oxiranyl)-acetic acid cyano-(6-methoxy-naphthalen-2-yl)-methyl ester.

* Corresponding author. Department of Applied Biological Science, Tokyo Noko University, 3-5-8 Saiwaicho, Fuchu, Tokyo, 183-8509, Japan.
E-mail address: hasumi@cc.tuat.ac.jp (K. Hasumi).

https://doi.org/10.1016/j.bbrc.2019.05.088
0006-291X/

2. Materials and methods

2.1. Materials

Mouse sEH was purified from mouse liver by affinity chromatography as described previously [15]. Recombinant human sEH (N-terminal His-tagged protein; item No. 10011669) was purchased from Cayman (Ann Arbor, MI, USA). 2'-[2-Benzothiazoyl]-6′-hydroxybenzothiazole phosphate (AttoPhos; Promega, Fitchburg, WI, USA) and (3-phenyl-oxiranyl)-acetic acid cyano-(6-methoxy-naphthalen-2-yl)-methyl ester (PHOME; Cayman) were used as substrates for N-phos and C-EH, respectively. *N*-substituted amino acids were obtained from commercial sources (*see*, Supplementary Table 1 for their supplier and non-abbreviated name).

2.2. Assay for N-phos

N-phos activity was assayed using a 96-well plate in buffer A (25 mM bis-Tris-HCl, pH 7.0, containing 1 mM $MgCl_2$ and 0.1 mg ml^{-1} bovine serum albumin). sEH (19.5 ng) was pre-incubated with or without an inhibitor for 10 min in 112 μl of buffer A at room temperature (20–25 °C). Subsequently, 37 μl of AttoPhos was added (final concentration at 15 μM; concentration was varied where indicated), and the reaction was allowed to proceed for 1 (for mouse sEH) or 3 h (for human sEH). Reaction was stopped by adding 75 μl 100 mM NaOH, then the fluorescent product formed was quantified (excitation, 435 nm; emission, 555 nm).

2.3. Assay for C-EH

sEH (12 ng) was preincubated with an inhibitor in 150 μl buffer A for 10 min at room temperature (20–25 °C). Subsequently, 50 μl 200 μM PHOME was added, and the fluorescent product formed was quantified kinetically for 30 min at 30 °C (excitation, 330 nm; emission, 465 nm).

2.4. Amino acid sequence comparison

The amino acid sequences of sEH were obtained from NCBI with the following RefSeq IDs: NP_001970.2 (human), XP_001163779.1 (chimpanzee), NP_031966.2 (mouse), NP_075225.1 (rat), XP_004848441.1 (naked mole rat), NP_001069002.1 (bovine), XP_005684099.1 (goat), NP_001001641.1 (pig), XP_001492725.1 (horse), XP_005635733.1 (dog), XP_003984847.1 (cat), XP_003412411.1 (elephant), XP_006884985.1 (elephant shrew), and XP_007936969.1 (aardvark).

3. Results and discussion

3.1. Screening for an N-Phos inhibitor

First, we tried to identify an N-phos selective inhibitor from natural sources. After screening of ~1000 microbial culture extracts, a fungal strain was found to contain an active substance, which was composed of tyrosine, proline, valine, and other unidentified components. However, the entire structure of the active substance has yet to be determined because of its low concentration,

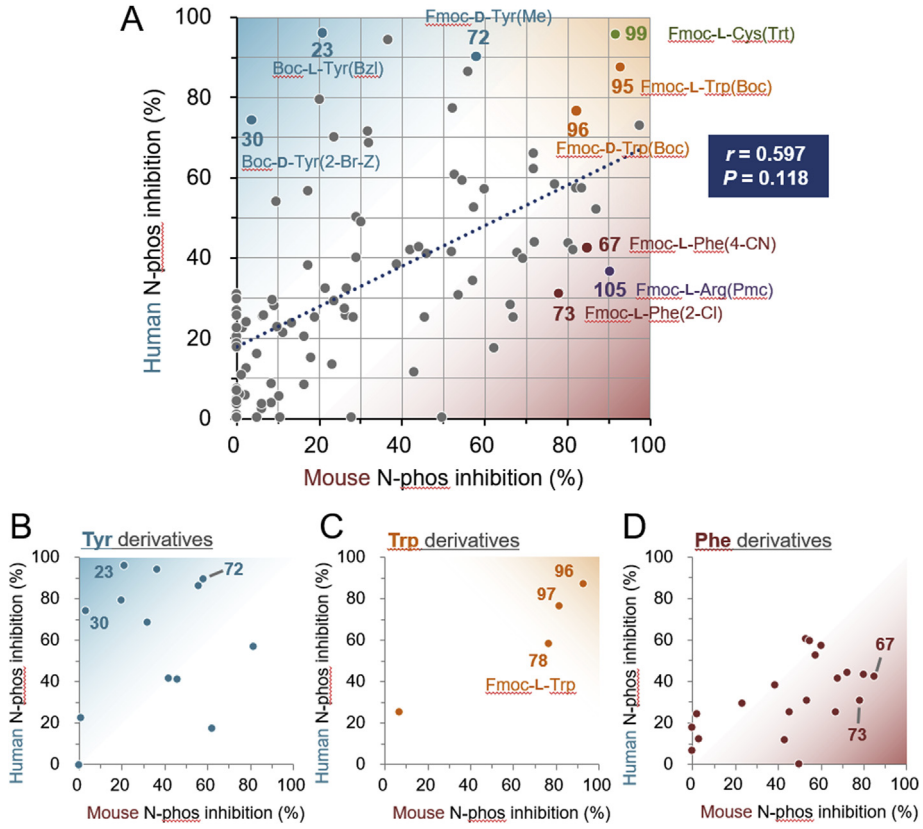

Fig. 1. Inhibition of N-phos in mouse and human sEH by *N*-substituted amino acids. (A) A plot of inhibition of mouse N-phos versus human N-phos, determined at the inhibitor concentrations at 6 and 30 μM, respectively. Dotted line represents regression curve for the correlation of inhibition between mouse and human N-phos. Pearson correlation coefficient (*r*) and probability value (*P*) are shown. (B–D) The data for tyrosine derivatives (B), tryptophan derivatives (C), and phenylalanine derivatives (D) are shown independently. Some potent compounds are labeled. Each value represents the mean from triplicate determinations.

suggesting high potency. Nevertheless, this results suggest that amino-acids or peptides could inhibit N-phos.

Therefore, a panel of available amino acids, peptides, and their derivatives were tested for their ability to inhibit N-phos. Although 33 free amino acids tested are essentially inactive, several corresponding *N*-substituted amino acids are inhibitory to N-phos in mouse sEH (32 out of the 109 tested *N*-substituted amino acids gave > 50% inhibition at 6 μM) (Fig. 1A and Supplementary Table 2). When *N*-substituted amino acids were tested for inhibition of the human N-phos, they appeared to be less potent than for inhibiting the murine enzyme. Therefore, we screened the compounds at higher concentrations for the human N-phos inhibitors. As a result, 27 out of the 109 tested *N*-substituted amino acids gave >50% inhibition at 30 μM (Fig. 1A and Supplementary Table 2).

3.2. Selectivity between mouse and human N-phos

Interestingly, many tyrosine derivatives, including Boc-L-Tyr(Bzl) (**23**) and Boc-D-Tyr(2-Br-Z) (**30**), are more potent on inhibiting the human N-phos than the mouse enzyme (Fig. 1B). Conversely, many phenylalanine derivatives, including Fmoc-L-Phe(4-CN) (**67**) and Fmoc-L-Phe(2-Cl) (**73**), are more potent on inhibiting the mouse N-phos than the human enzyme (Fig. 1D). Only a few compounds, such as tryptophan derivatives, Fmoc-L-Trp (**78**), Fmoc-L-Trp(Boc) (**95**), and Fmoc-D-Trp(Boc) (**96**), are inhibitory to N-phos of both species (Fig. 1C). Indeed, no correlation was found between the mouse and human N-phos inhibition data obtained with the 109 test compounds ($r = 0.597$; $P = 0.118$) (Fig. 1A).

The great variance in the N-phos inhibition by *N*-substituted amino acids suggests differences in the catalytic site structure between mouse and human N-phos.

3.3. Selectivity between N-Phos and C-EH

Compounds with >75% inhibition of mouse N-phos at 6 μM were tested for inhibition of the mouse C-EH (Supplementary Table 3). Among the 14 compounds tested (**27**, **67**, **73**, **78**, **79**, **82**, **83**, **84**, **85**, **95**, **96**, **99**, **104**, and **105**), Fmoc-L-Phe(4-CN) (**67**) and Fmoc-L-Trp (**78**) are relatively potent for N-phos (Fig. 2A). IC_{50} values of **67** for N-phos and C-EH in mouse sEH were 2.3 and 85 μM, respectively, with a selectivity index of 37, and those of **78** were 4.0 and ~200 μM, respectively (selectivity index ~50). Because N-phos and C-EH inhibition by ebselen are time dependent [13], the effect of time was also investigated. Both **67** and **78** did not display any time-dependent change in C-EH inhibition in the time-window tested (1.7–120 min).

Compounds with >72% inhibition of human N-phos at 30 μM (**23**, **26**, **29**, **30**, **72**, **76**, **84**, **95**, **96**, **98**, **99**, and **100**) were tested for inhibition of human C-EH (Supplementary Table 3). Boc-L-Tyr(Bzl) (**23**) and Fmoc-D-Tyr(Me) (**72**) were found to be relatively potent for N-phos (Fig. 2B). IC_{50} values of **23** for N-phos and C-EH in human sEH were 1.5 and 190 μM, respectively (selectivity index = 127), and those of **72** were 6.5 and > 200 μM, respectively (selectivity index >31). Both compounds showed no time-dependent change in C-EH inhibition.

AFC has been shown to selectively inhibit N-phos in human sEH

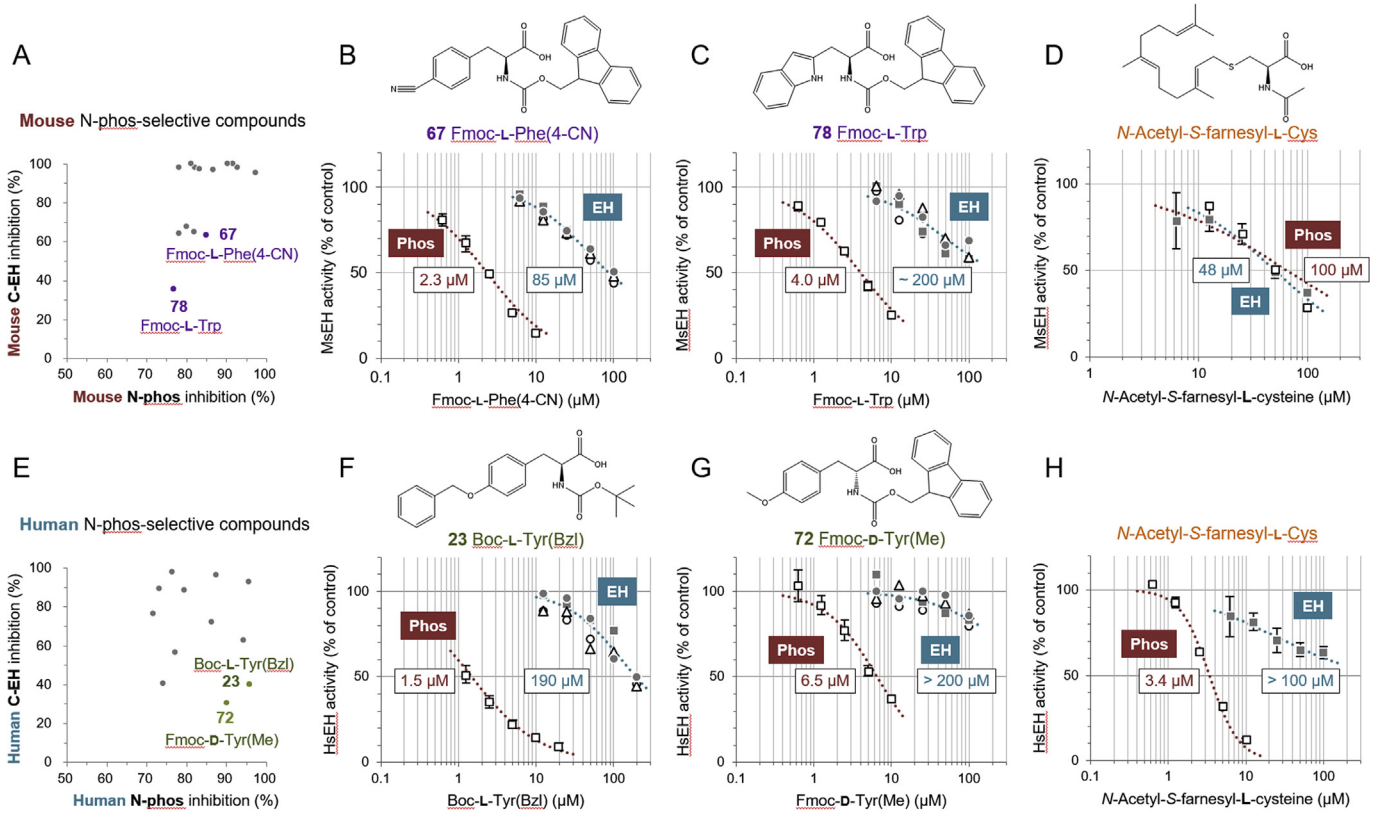

Fig. 2. Identification of N-phos-selective inhibitors potent for mouse or human sEH. (A) A plot of inhibition of N-phos versus C-EH in mouse sEH, determined at the inhibitor concentrations at 6 and 200 μM, respectively. (B–D) Effects of Fmoc-L-Phe(4-CN) (**67**), Fmoc-L-Trp (**78**), and *N*-acetyl-*S*-farnesyl-L-cysteine (AFC) on N-phos and C-EH in mouse sEH. (E) A plot of inhibition of N-phos versus C-EH in human sEH, determined at the inhibitor concentrations at 30 and 200 μM, respectively. (F–H) Effects of Boc-L-Tyr(Bzl) (**23**), Fmoc-D-Tyr(Me) (**72**), and AFC on N-phos and C-EH in human sEH. In B, C, F, and G, C-EH activity was determined after preincubation with the inhibitor for 1.7 (open circle), 10 (closed square), 30 (open triangle), and 120 min (closed circle). Each value represents the mean ± SD from triplicate determinations.

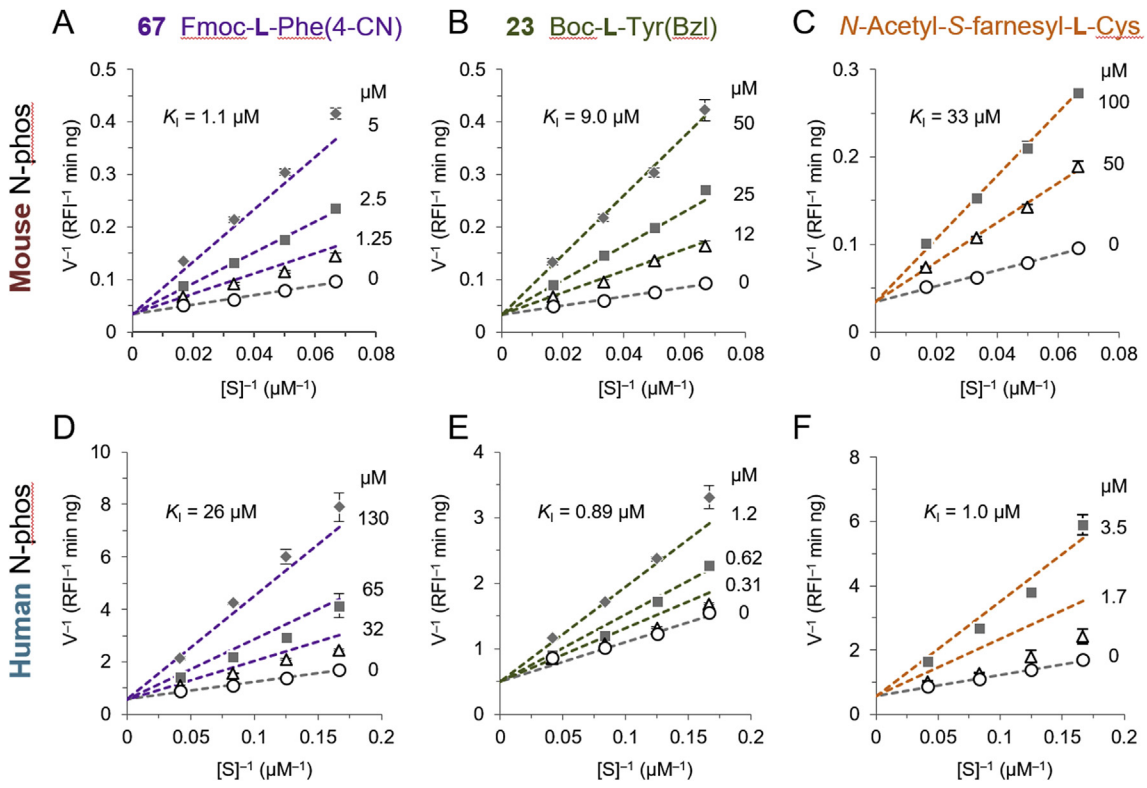

Fig. 3. Kinetic analysis of the inhibition of mouse and human N-phos. (A–C) Kinetics of the inhibition of mouse N-phos by Fmoc-L-Phe(4-CN) (**67**), Boc-L-Tyr(Bzl) (**23**), and *N*-acetyl-*S*-farnesyl-L-cysteine (AFC). (D–F) Kinetics of the inhibition of mouse N-phos by **67**, **23**, and AFC. Each value represents the mean ± SD from triplicate determinations. Dotted line represents the theoretical line derived from the model of competitive inhibition fitted to the experimental data. K_I value is shown in each panel. K_S and V_{MAX} values, respectively, were: 26 μM and 29 relative fluorescence intensity (RFI) min^{-1} ng^{-1} for mouse *N*-phos; and 11 μM and 1.7 RFI min^{-1} ng^{-1} for human N-phos.

[7]. Our results are consistent with the reported data with respect to the inhibition of human sEH: IC_{50} values of AFC for N-phos and C-EH in human sEH were 3.4 and > 100 μM, respectively (selectivity index >29) (Fig. 2B). However, the pattern of its inhibition of mouse sEH was quite different from that of human sEH inhibition (Fig. 2A); AFC inhibited mouse C-EH (IC_{50} 48 μM) more strongly than N-phos (IC_{50} 100 μM). Our results suggest great caution should be taken in interpreting data when using AFC to inhibit N-phos in mouse.

3.4. Inhibition kinetics

Inhibition mechanism for mouse N-phos (**67**) and human N-phos (**23**) were characterized kinetically (Fig. 3). Both compounds inhibited N-phos in mouse and human sEH competitively with respect to the substrate AttoPhos. K_I values for mouse and human N-phos were 1.1 and 26 μM, respectively, for **67** (24-fold preference for mouse N-phos) and 9.0 and 0.89 μM, respectively, for **23** (10-fold preference for human N-phos). Similarly, AFC competitively inhibited N-phos in mouse and human sEH, whereas inhibition of mouse N-phos was much weaker than that of human N-phos ($K_I = 33$ and 1.1 μM, respectively).

Taken together, our investigation led to the identification of competitive inhibitors showing specificity for the N-phos in mouse or human sEH. Compound **67** is specific for mouse N-phos (37-fold over mouse C-EH and 24-fold over human N-phos), and **23** is specific for human N-phos (127-fold over human C-EH and 10-fold over mouse N-phos). These results strongly suggest a substantial difference between mouse N-phos and human N-phos in the recognition of a ligand, either inhibitor or substrate.

3.5. Interspecies diversity in the catalytic pocket structure

Fig. 4A depicts the catalytic pocket structures of N-phos and C-EH in human sEH. The amino acids D9, D11, T123, N124, K160, D184, D185, and N189 are lining the N-phos active site and play some roles in the N-phos catalysis [18]. The amino acids Asp335, Asp496, and His524, which form the catalytic triad, as well as Tyr383 and Tyr466, which act as acid catalysts, are crucial in human C-EH activity [19,20]. It should be noted that some amino acid numberings are different from those in the reference because of the difference of the reference sequence; the numbering in this work is based on RefSeq ID NP_001970.2. Amino acid residues that form the catalytic pocket surface (<10 Å from the catalytic groups) in N-Phos or C-EH were compared among 14 different mammalian species (Fig. 4B). Overall, across species there is far more variation in the N-terminal domain of sEH than in its C-terminal domain. Notably, 8 of the 23 surface residues in the N-phos catalytic pocket in human sEH (V19, F20, F41, T51, T125, V159, I186, and A188) are changed in mouse sEH (to I, A, Y, E, N, I, and F, respectively). These changes may account for the great interspecies variation of the N-phos inhibition by *N*-substituted amino acids. On the other hand, only 3 of the 20 surface residues in the C-EH catalytic pocket in human sEH (M339, L408, and M419) are changed in mouse sEH (to V, F, and A, respectively).

The amino acid positions at V19, F20, T50, T51, V159, I186, and A188 in human N-phos are particularly divergent among the 14 mammalian species examined (Fig. 4B). Moreover, D9, D11 and D185, which play significant role in the N-Phos catalysis [18], are not fully conserved, suggesting a mild selection pressure during the evolutionary history of N-phos. The variation in the N-phos catalytic pocket structure along with the interspecies difference in

A

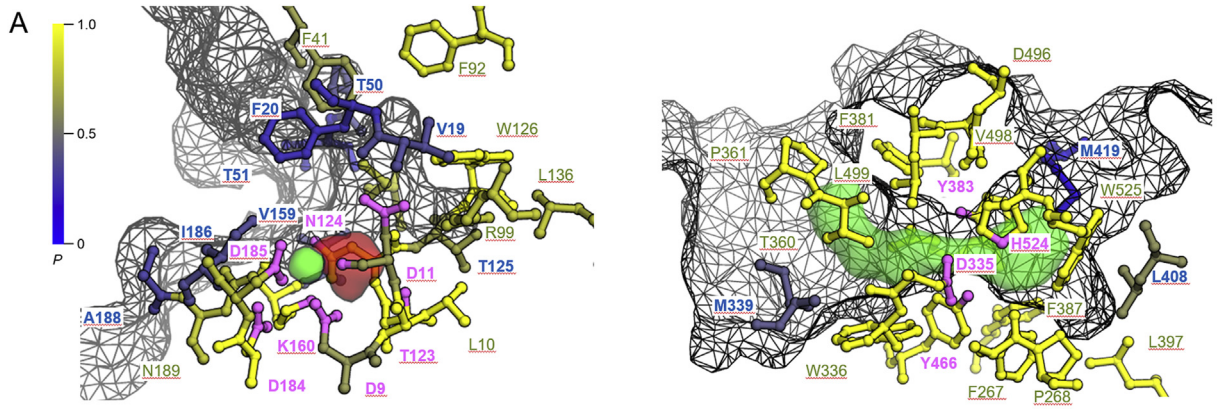

B

Residue No.	9	10	11	19	20	41	50	51	54	92	99	123	124	125	126	136	159	160	184	185	186	188	189	267	268	335	336	339	360	361	381	383	384	387	397	408	419	466	496	498	499	524	525
Human	D	L	D	V	F	F	T	T	M	F	R	T	N	T	W	L	V	K	D	D	I	A	N	F	P	D	W	M	T	P	F	Y	Q	F	L	L	M	Y	D	V	L	H	W
Chimpanzee	D	L	D	V	F	F	T	T	M	F	R	T	N	T	W	L	V	K	D	D	I	A	N	F	P	D	W	M	T	P	F	Y	Q	F	L	L	M	Y	D	V	L	H	W
Mouse	D	L	D	I	A	Y	T	E	M	F	R	T	N	N	W	L	I	K	D	D	F	S	N	F	P	D	W	V	T	P	F	Y	Q	F	L	F	A	Y	D	V	L	H	W
Rat	D	L	D	I	A	F	T	E	M	F	R	T	N	N	W	L	I	K	D	D	F	S	N	F	P	D	W	V	T	P	F	Y	Q	F	L	F	T	Y	D	V	L	H	W
Naked mole rat	E	L	D	V	A	F	S	G	M	F	R	T	N	N	W	L	V	K	D	D	F	S	N	F	P	D	W	V	T	P	F	Y	Q	F	L	F	P	Y	D	V	L	H	W
Bovine	E	L	G	A	T	F	S	I	M	F	R	T	N	T	W	L	V	K	D	N	F	T	N	F	P	D	W	M	T	P	F	Y	Q	F	L	F	T	Y	D	V	L	H	W
Goat	D	L	V	V	T	F	S	T	M	F	R	T	N	N	W	M	V	K	D	N	F	T	N	F	P	D	W	M	T	P	F	Y	Q	F	L	F	T	Y	D	V	L	H	W
Pig	D	L	D	I	T	F	V	A	M	F	K	T	N	N	W	R	A	K	D	D	V	T	H	F	P	D	W	V	T	P	F	Y	Q	F	L	F	T	Y	D	V	L	H	W
Horse	D	L	D	I	A	L	I	A	V	F	R	T	N	N	W	L	A	K	D	D	I	A	Y	F	P	D	W	M	T	P	F	Y	Q	F	L	F	S	Y	D	V	L	H	W
Dog	D	L	D	V	V	S	S	A	M	F	R	T	N	N	W	L	A	K	D	D	I	A	N	F	P	D	W	M	T	P	F	Y	Q	F	L	F	N	Y	D	V	L	H	W
Cat	D	L	Y	L	A	F	S	A	M	F	K	T	N	N	W	L	A	K	D	D	I	A	N	F	P	D	W	M	T	P	F	Y	Q	F	L	F	S	Y	D	V	L	H	W
Elephant	S	L	D	I	A	F	S	A	I	F	R	T	N	N	W	L	A	K	D	D	T	A	N	F	P	D	W	L	T	P	F	Y	Q	F	L	L	S	Y	D	V	L	H	W
Elephant shrew	D	L	D	V	F	F	T	V	M	F	R	T	N	N	W	L	V	K	D	D	F	S	N	F	P	D	W	A	T	P	F	Y	Q	F	L	F	-	Y	D	V	L	H	W
Aardvark	D	L	D	I	L	F	S	V	M	M	R	T	N	N	W	L	A	K	D	D	I	T	N	F	P	D	W	M	T	P	F	Y	Q	F	L	L	-	Y	D	V	L	H	W
P value	0.62	1.00	0.60	0.33	0.23	0.60	0.34	0.16	0.73	0.86	0.74	1.00	1.00	0.64	1.00	0.73	0.34	1.00	1.00	0.74	0.33	0.30	0.73	1.00	1.00	1.00	1.00	0.37	1.00	1.00	1.00	1.00	1.00	1.00	1.00	0.56	0.12	1.00	1.00	1.00	1.00	1.00	1.00

Fig. 4. The catalytic pocket structure of N-phos and C-EH. (A) The catalytic pocket structure of human sEH based on PDB 1ZD5. Amino acid residues that form a molecular surface (*mesh*) within 10 Å from the catalytically essential groups (*pink*) are shown as balls-and-sticks, which are variably colored based on their *P* values (*left bar*). Small molecule ligands in the crystal structure are shown as space-filling models: magnesium ion (green) and phosphoric ion (red) in the active site of N-phos (*left*); and 4-(3-cyclohexylureido)-heptanoic acid (green) in the active site of C-EH (*right*). (B) Amino acid sequences of sEH from 14 different mammalian species are aligned based on the sequence of human sEH. *P* value represents a probability of two randomly selected sequences to fall into an identical amino acid at each position. The amino acid residues that are different between the human and mouse sequences are colored in the mouse sequence. (For interpretation of the references to color in this figure legend, the reader is referred to the Web version of this article.)

inhibition by *N*-substituted amino acids suggests a high variability in substrate preference for N-phos among mammalian species. In the same context, species-selective information is required in the use of an inhibitor of N-phos.

Put together, our results show that amino acid derivatives are good inhibitors of sEH N-phos across species. However, high variability in the N-term sequence results in divergent inhibitor selectivity among species, suggesting caution when targeting N-phos in animal models.

Conflicts of interest

KH is a board member of TMS Co., Ltd., Tokyo, Japan, which provided collaborative research expenses.

Funding

This study was supported in part by a grant from the Japan Society for the Promotion of Science (17H02201 to KH) and Grant # ES002710 from the National Institute of Environmental Health Sciences (NIEHS).

Acknowledgments

We thank Professor Kit Lam for providing amino acid derivatives.

Appendix A. Supplementary data

Supplementary data to this article can be found online at https://doi.org/10.1016/j.bbrc.2019.05.088.

Transparency document

Transparency document related to this article can be found online at https://doi.org/10.1016/j.bbrc.2019.05.088.

References

[1] T.R. Harris, B.D. Hammock, Soluble epoxide hydrolase: gene structure, expression and deletion, Gene 526 (2013) 61–74.
[2] K.M. Wagner, C.B. McReynolds, W.K. Schmidt, B.D. Hammock, Soluble epoxide hydrolase as a therapeutic target for pain, inflammatory and neurodegenerative diseases, Pharmacol. Ther. 180 (2017) 62–76.
[3] K. Hashimoto, Role of soluble epoxide hydrolase in metabolism of PUFAs in psychiatric and neurological disorders, Front. Pharmacol. 10 (2019) 36.
[4] A. Oguro, S. Imaoka, Lysophosphatidic acids arenew substrates for the phosphatase domain of soluble epoxide hydrolase, J. Lipid Res. 53 (2012) 505–512.
[5] C. Morisseau, N.H. Schebb, H. Dong, A. Ulu, P.A. Aronov, B.D. Hammock, Role of soluble epoxide hydrolase phosphatase activity in the metabolism of lysophosphatidic acids, Biochem. Biophys. Res. Commun. 419 (2012) 796–800.
[6] K.L. Tran, P.A. Aronov, H. Tanaka, J.W. Newman, B.D. Hammock, C. Morisseau, Lipid sulfates and sulfonates are allosteric competitive inhibitors of the N-terminal phosphatase activity of the mammalian soluble epoxide hydrolase, Biochemistry 44 (2005) 12179–12187.
[7] A.E. EnayetAllah, D.F. Grant, Effects of human soluble epoxide hydrolase polymorphisms on isoprenoid phosphate hydrolysis, Biochem. Biophys. Res.

Commun. 341 (2006) 254–260.
[8] H.-H. Hou, B.D. Hammock, K.-H. Su, C. Morisseau, Y.R. Kou, S. Imaoka, A. Oguro, S.-K. Shyue, J.-F. Zhao, T.-S. Lee, N-terminal domain of soluble epoxide hydrolase negatively regulates the VEGF-mediated activation of endothelial nitric oxide synthase, Cardiovasc. Res. 93 (2012) 120–129.
[9] H.-H. Hou, Y.-J. Liao, S.-H. Hsiao, S.-K. Shyue, T.-S. Lee, Role of phosphatase activity of soluble epoxide hydrolase in regulating simvastatin-activated endothelial nitric oxide synthase, Sci. Rep. 5 (2015) 13524.
[10] A.E. EnayetAllah, A. Luria, B. Luo, H.J. Tsai, P. Sura, B.D. Hammock, D.F. Grant, Opposite regulation of cholesterol levels by the phosphatase and hydrolase domains of soluble epoxide hydrolase, J. Biol. Chem. 283 (2008) 36592–36598.
[11] A. Luria, C. Morisseau, H.-J. Tsai, J. Yang, B. Inceoglu, B. De Taeye, S.M. Watkins, M.M. Wiest, J.B. German, B.D. Hammock, Alteration in plasma testosterone levels in male mice lacking soluble epoxide hydrolase, Am. J. Physiol. Endocrinol. Metab. 297 (2009) E375–E383.
[12] J. Kramer, E. Proschak, Phosphatase activity of soluble epoxide hydrolase, Prostag. Other Lipid Mediat. 133 (2017) 88–92.
[13] C. Morisseau, S. Sahdeo, G. Cortopassi, B.D. Hammock, Development of an HTS assay for EPHX2 phosphatase activity and screening of nontargeted libraries, Anal. Biochem. 434 (2013) 105–111.
[14] F.-M. Klingler, M. Wolf, S. Wittmann, P. Gribbon, E. Proschak, Bacterial expression and HTS assessment of soluble epoxide hydrolase phosphatase, J. Biomol. Screen 21 (2016) 689–694.
[15] N. Matsumoto, E. Suzuki, M. Ishikawa, T. Shirafuji, K. Hasumi, Soluble epoxide hydrolase as an anti-inflammatory target of the thrombolytic stroke drug SMTP-7, J. Biol. Chem. 289 (2014) 35826–35838.
[16] N. Matsumoto, E. Suzuki, K. Tsujihara, Y. Nishimura, K. Hasumi, Structure-activity relationships of the plasminogen modulator SMTP with respect to the inhibition of soluble epoxide hydrolase, J. Antibiot. 68 (2015) 685–690.
[17] S. Otake, N. Ogawa, Y. Kitano, K. Hasumi, E. Suzuki, Isoprene side-chain of SMTP is essential for soluble epoxide hydrolase inhibition and cellular localization, Nat. Prod. Commun. 11 (2016) 223–227.
[18] A. Cronin, S. Homburg, H. Dürk, I. Richter, M. Adamska, F. Frère, M. Arand, Insights into the catalytic mechanism of human sEH phosphatase by site-directed mutagenesis and LC-MS/MS analysis, J. Mol. Biol. 383 (2008) 627–640.
[19] M. Arand, H. Wagner, F. Oesch, Asp333, Asp495, and His523 form the catalytic triad of rat soluble epoxide hydrolase, J. Biol. Chem. 271 (1996) 4223–4229.
[20] K.H. Hopmann, F. Himo, Insights into the reaction mechanism of soluble epoxide hydrolase from theoretical active site mutants, J. Phys. Chem. B 110 (2006) 21299–21310.